

Viscoelastic Properties of Bulk Groundnuts

¹K.V. Too, ¹E.B.K. Mutai, ¹J.M. Mutua, ¹D.A. Mutuli and ²D.O. Mbuge

¹Department of Environmental and Biosystems Engineering, University of Nairobi,
School of Engineering, P.O. BOX 30197, Code 00100, Nairobi, Kenya

²Department of Biomechanical and Environmental Engineering, Jomo Kenyatta University of
Agriculture and Technology, P.O. BOX 62000, Code 00200, Nairobi

Abstract: The groundnut, *Arachis hypogaea* Linn, samples were collected from the majorly grown areas of western Kenya to investigate the viscoelastic properties pertinent to grain handling, storage and processing. In particular, the study conducted at the University of Nairobi, Department of Environmental and Biosystems laboratories in July 2010, aimed at investigating the stress-strain properties of bulk groundnuts in relation to Maxwell polymer viscoelastic model. The Mohr-Coulomb failure criterion was also applied to bulk groundnuts. Three samples were prepared for triaxial tests; each weighing 1062.4 g. The moisture content of the samples was 7.6%. The sample size for triaxial testing was 100 mm diameter and 199 mm height. Density of the samples during the tests was 678.6 kg/m³. Confining stresses of 200, 400 and 600 kPa were used and Axial Strain Rate (ASR) of 0.5 mm/min was used for the triaxial compression tests. For the senstar universal testing machine relaxation time was about 30 min for each of the samples. Relaxation data was recorded after every 30 sec for the duration of the test (30 min). These results showed that the Maxwell model for viscoelastic polymers can be applied to accurately describe the behaviour of bulk groundnuts.

Key words: *Arachis hypogaea* Linn, compression tests, creep, relaxation time, strain, stress, triaxial tests, viscoelasticity

INTRODUCTION

Scientific studies of granular materials date back to as early as the 18th Century (Goldhirsch and Goldenberg, 2004). Even though granular materials testing was initially restricted to only materials of engineering significance such as engineering construction materials, theories developed are fast gaining entry into the agricultural food and processing industry globally.

Groundnuts are grown by peasant farmers in Western Kenya for local consumption. The planting, harvesting and most of the post harvesting operations are carried out manually. In view of the fact that the design of some of the cultivation machinery such as mechanical planters and processing equipment are dependent on some mechanical properties of the groundnuts, consequently it is necessary to evaluate such properties for local varieties. There is need to consider such properties when designing farm machinery and processing equipment. Aggrawal *et al.* (1973), Ndukwu (2009) and Oranga (2005) have indicated that many studies have been done in the recent past on agricultural products and fruits. In this regard, groundnuts

form one of the most important cereal crops and therefore one of the most significant types of granular materials.

In the 19th century, physicists such as Maxwell, Boltzmann, and Kelvin researched and experimented with creep and recovery of glasses, metals, and rubbers (McCrum *et al.*, 2003). Viscoelasticity was further examined in the late twentieth century when synthetic polymers were engineered and used in a variety of applications. Viscoelasticity calculations depend heavily on the viscosity variable, η . The inverse of η is also known as fluidity, ϕ . The value of either can be derived as a function of temperature or as a given value (i.e., for a dashpot), (Meyers and Chawla, 1999):

Viscoelasticity is the property of materials that exhibit both viscous and elastic characteristics when undergoing deformation. Viscous materials, like honey, resist shear flow and strain linearly with time when a stress is applied. Elastic materials strain instantaneously when stretched and just as quickly return to their original state once the stress is removed. Viscoelastic materials have elements of both of these properties and, as such, exhibit time dependent strain. Whereas elasticity is

usually the result of bond stretching along crystallographic planes in an ordered solid, viscoelasticity is the result of the diffusion of atoms or molecules inside of an amorphous material (Moya *et al.*, 2002, 2006).

Objectives: The overall objective of the study was to evaluate the constitutive relations of groundnuts, especially rheological properties. The specific objectives were:

- To establish the stress-strain viscoelastic parameters of bulk groundnuts based on Maxwell model and to establish the Mohr-Coulomb failure constants and
- To experiment the time dependent behavior of groundnut under quasi-static state, that is:
 - Instantaneous elasticity
 - Creep under constant stress and
 - Stress relaxation under constant strain

Triaxial testing of granular agricultural material: The most widely used laboratory equipment for investigating the stress-strain behaviour of granular soils is the triaxial apparatus (Chi *et al.*, 1993). Over time, this equipment has been modified to test the stress-strain relationship of granular agricultural materials. Modification has therefore been done for the triaxial test apparatus to model elastoviscoplastic stress-strain behaviour of bulk wheat. The versatility of the triaxial equipment enabled it to perform both the cyclic and monotonic tests. Later, Zhang *et al.* (1998) used the triaxial equipment in the

determination of stress-strain and volume-strain behaviour of soybean. Similar application of the equipment have also been reported by Gumbe and Maina (1990) who used it to test the elastoplastic behaviour of rice *en masse* and Zhang *et al.* (1986, 1989a) for wheat *en masse*. Also triaxial test machine was used by Oranga (2005) to test elastoviscoplastic behavior of maize *en masse*. The above studies emanated from the realization that all granular matter has some unique defining characteristics which makes it possible to categorize them as continuum.

Senstar testing of granular materials: The Senstar Universal Testing (SUT) machine is standard equipment used in the field of engineering mechanics and in the study of the behaviour of food and agricultural materials especially under uniaxial loading conditions. For example, Ak and Gunasekaran (1992) used the instron equipment in testing the stress-strain properties of cheese under uniaxial compression loading. The instron equipment, in its standard form, performs both cyclic and monotonic loading tests. (Oranga, 2005)

MATERIALS AND METHODS

Sample collection and preparation: The groundnut, *Arachis hypogaea* Linn, sample was collected from the majorly grown areas of western Kenya (Kakamega). The sample was packaged in a packet of 1 kg each and sealed to maintain moisture content. Experiments were conducted in July 2010 at the University of Nairobi,

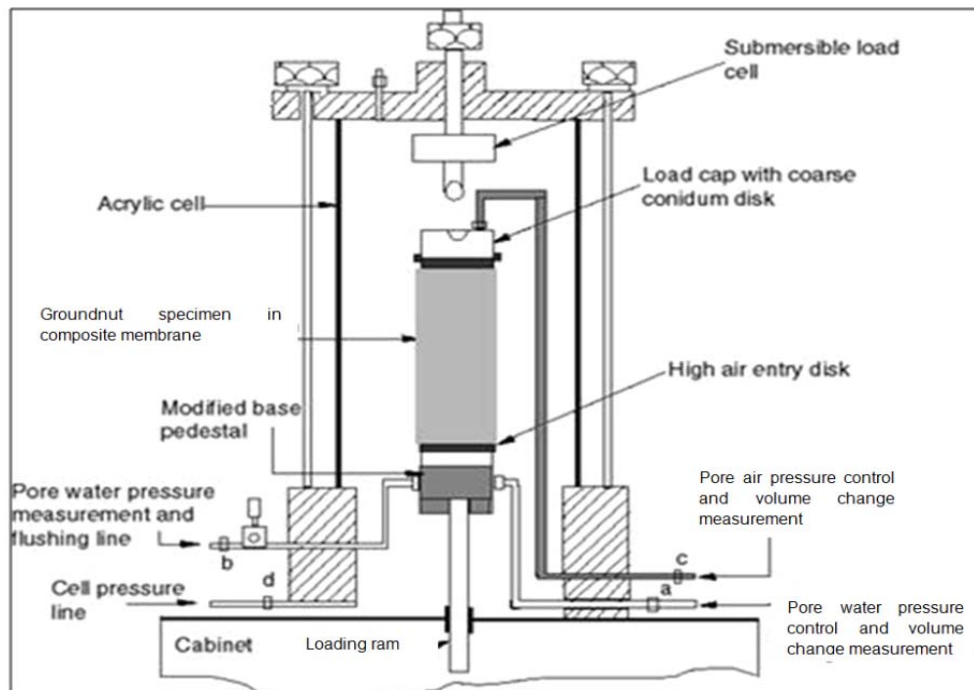


Fig. 1: Modified triaxial test device for compression loading

Department of Environmental and Biosystems Laboratories at Kabete Campus.

Sample preparation for triaxial testing: Three samples were prepared for triaxial tests, each weighing 1062.4 g. The moisture content of the samples was determined using the moisture content meter and found to be 7.6%. The sample size for triaxial testing was 100 mm diameter and 199 mm height. Density of the samples during the tests was 678.6 kg/m³

Equipment description:

Triaxial testing equipment: Figure shows a schematic diagram of the triaxial testing equipment used for the triaxial compression loading experiments (Oranga, 2005). The triaxial cell was designed and built by ELE International (Eastman way, UK). Standard triaxial testing procedures proposed by Bishop and Henkel (1962) were modified as suggested by Wang *et al.* (2002); and Zhang *et al.* (1998) for testing of unsaturated granular agricultural materials. The quantities that were measured during the tests included the stress transmitted by the cell fluid (air), the axial force applied to the loading ram and the change in length of the sample. To control pore pressure, the pore pressure channels were closed throughout the tests.

Cell pressure: is the confining stress inside the acrylic cell. It is usual to apply some fluid (normally air or water) as a medium of exerting the stress. Due to its compressibility, air pressure was applied in the experiments in this research (Oranga, 2005).

The cell pressure provided the all round stress on the sample giving the minor principal stress (σ_3). To ensure that a constant minor principal stress was maintained throughout the tests, the cell pressure line shown in Fig. 1 was connected to a compressor vessel.

Axial stress: is the axial force applied to the loading ram which depended on the above cell stresses since these had to be overcome during the tests for effective stress to be registered. (Oranga, 2005)

Pore pressure: is the pressure in the pore fluid (air, water or both air and water) and plays an important role in triaxial tests (Wood, 1990). With the assumption of incompressibility of air and in the case of Unconsolidated Undrained (UU) tests as the one conducted, these pressure channels were closed. The alternative tests i.e., Consolidate Drained (Cd) or the Consolidated Undrained (CU) tests would require the opening of the channels.

Materials Testing: Confining stresses of 200, 400 and 600 kPa were used and axial strain rate (ASR) of 0.5 mm/min used for the triaxial compression tests.

Triaxial tests: All triaxial tests included two stages, isotropic consolidation and axial compression. The purpose of the isotropic consolidation stage was to allow stabilization of volume change (Zhang *et al.*, 1998) and of confining stress. After the isotropic consolidation stage, the vertical loading system was turned on. The axial force was increased by compressing the sample at predetermined displacement rate of 0.5 mm/min until the test was terminated at failure. The triaxial test cycle therefore consisted of the following four stages namely consolidation stage, compression stage, shear along an axis and finally failure of the sample (Oranga, 2005).

For each applied load, the axial unit strain (ϵ) was computed by dividing the change in length (Δl) of the specimen, by the initial length (l_0) of the specimen:

$$\epsilon = \Delta l/l_0 \tag{1}$$

Each corresponding cross-sectional area (A) of the specimen was computed from:

$$A = A_0/1 - \epsilon \tag{2}$$

where, A_0 is the initial cross-sectional area of the specimen.

Each corresponding axial load was determined by multiplying the proving ring dial reading by the proving ring calibration. Finally, each unit axial load was computed by dividing each applied axial load by the corresponding cross sectional area, for each specimen tested. The mean or equivalent stress, σ_m , was computed from:

$$\sigma_m = (\sigma_1 + 2\sigma_3)/3 \tag{3}$$

where, σ_1 , and, σ_3 are the applied axial stress and confining stress respectively.

Creep test: To determine creep properties, the material was subjected to prolonged constant compression loading at constant elevated temperature. Deformation was recorded at specified time intervals and a creep vs. time diagram was plotted. Slope of curve at any point was creep rate. Failure occurrence terminated the test and the time for rupture was recorded.

Stress-relaxation tests: The material prepared as described blow was carefully loaded on the SUT equipment using a plunger to a strain level of 15%. The strain was then fixed to this point as the monitoring of stress-relaxation of the material began. Relaxation time was about 30 min for each of the samples. Relaxation data was recorded after every 30 sec for the duration of the test (30 min).

Table 1: Triaxial tests at 200 kpa

Elapsed time	Deformation		Cross-sectional area (mm ²)	Proving ring dial	Applied axial (N)	Unit axial load (kpa)
	Dial, ΔL	Axial strain,				
At 200 kpa, Initial height: 160mm;						
0	0.0	0	7854.000	0	0	0
1.07	0.5	0.0031	7878.62	5	150	19.039
2.56	1.0	0.0063	7903.40	10	300	37.958
4.22	1.5	0.0094	7928.33	17	510	64.326
5.25	2.0	0.0125	7953.42	26	780	98.071
6.26	2.5	0.0156	7978.67	30	900	112.80
7.26	3.0	0.01888	004.080	37	1110	138.68
8.22	3.5	0.0219	8029.65	39	1170	145.71
9.21	4.0	0.0250	8055.38	42	1260	156.42
10.19	4.5	0.0281	8081.29	45	1350	167.05
11.14	5.0	0.0313	8107.35	47	1410	173.92
12.14	5.5	0.0344	8133.59	49	1470	180.73
13.26	6.0	0.0375	8160.00	52	1560	191.18
14.46	6.5	0.0406	8186.58	55	1650	201.55
15.41	7.0	0.0438	8213.33	58	1740	211.85
16.41	7.5	0.0469	8240.26	60	1800	218.44
17.4	8.0	0.0500	8267.37	63	1890	228.61
18.35	8.5	0.0531	8294.65	64	1920	231.47
19.34	9.0	0.0563	8322.12	65	1950	234.32
20.32	9.5	0.0594	8349.77	66	1980	237.13
21.28	10.0	0.0625	8377.60	67	2010	239.93
22.3	10.5	0.0656	8405.62	69	2070	246.26
22.44	11.0	0.0688	8433.83	68	2040	241.88
24.51	11.5	0.0719	8462.22	68	2040	241.07
25.52	12.0	0.0750	8490.81	68	2040	240.26
26.51	12.5	0.0781	8519.59	70	2100	246.49
27.48	13.0	0.0813	8548.57	70	2100	245.66
28.44	13.5	0.0844	8577.75	70	2100	244.82
29.44	14.0	0.0875	8607.12	69	2070	240.50
30.41	14.5	0.0906	8636.70	69	2070	239.67
31.36	15.0	0.0938	8666.48	69	2070	238.85
32.36	15.5	0.0969	8696.47	69	2070	238.03
33.46	16.0	0.1000	8726.67	68	2040	233.77
34.58	16.5	0.1031	8757.07	68	2040	232.95
35.57	17.0	0.1063	8787.69	68	2040	232.14
36.55	17.5	0.1094	8818.53	67	2010	227.93
Proving ring calibration: 30N/m²						
0	0.0	0	7854.000000	0	0	0
1.05	0.5	0.002564	7874.190231	6	180	22.85949345
2.06	1.0	0.005128	7894.484536	7	210	26.60085013
3.16	1.5	0.007692	7914.883721	9	270	34.11294588
4.54	2.0	0.010256	7935.388601	9	270	34.02479873
5.37	2.5	0.012821	7956.000000	9	270	33.93665158
7.11	3.0	0.015385	7976.718750	16	480	60.17511900
8.11	3.5	0.017949	7997.545692	38	1140	142.5437308
9.11	4.0	0.020513	8018.481675	38	1140	142.1715539
10.1	4.5	0.023077	8039.527559	47	1410	175.3834401
11.09	5.0	0.025641	8060.684211	56	1680	208.4190319
12.11	5.5	0.028205	8081.952507	65	1950	241.2783295
13.21	6.0	0.030769	8103.333333	74	2220	273.9613328
14.1	6.5	0.033333	8124.827586	82	2460	302.7756557
15.4	7.0	0.035897	8146.436170	88	2640	324.0680888
16.41	7.5	0.038462	8168.160000	92	2760	337.8973967
17.39	8.0	0.041026	8190.000000	97	2910	355.3113553
18.34	8.5	0.043590	8211.957105	99	2970	361.6677440
19.31	9.0	0.046154	8234.032258	102	3060	371.6283716
20.29	9.5	0.048718	8256.226415	106	3180	385.1638558
21.25	10.0	0.05128282	78.54054100	108	3240	391.3733325
22.27	10.5	0.053846	8300.975610	111	3330	401.1576659
23.35	11.0	0.056410	8323.532609	113	3390	407.2789955
24.5	11.5	0.058974	8346.212534	114	3420	409.7667039
25.5	12.0	0.061538	8369.016393	116	3480	415.8194746

Table 1: (Continue)

Elapsed time	Deformation		Cross-sectional area (mm ²)	Proving ring dial	Applied axial (N)	Unit axial load (kpa)
	Dial, ΔL	Axial strain,				
26.5	12.5	0.064103	8391.945205	116	3480	414.6833559
27.46	13.0	0.066667	8415.000000	116	3480	413.5472371
28.43	13.5	0.069231	8438.181818	116	3480	412.4111183
29.4	14.0	0.071795	8461.491713	116	3480	411.2749995
30.37	14.5	0.074359	8484.930748	115	3450	406.6032007
31.32	15.0	0.076923	8508.500000	114	3420	401.9509902
32.34	15.5	0.079487	8532.200557	113	3390	397.3183679
33.39	16.0	0.082051	8556.033520	112	3360	392.7053339
34.54	16.5	0.084615	8580.000000	111	3330	388.1118881

Table 2: Triaxial tests at 400 kpa

Elapsed time	Deformation		Cross-sectional area (mm ²)	Proving ring dial	Applied axial (N)	Unit axial load (kpa)
	dial, ΔL	Axial strain,				
0	0.0	0	7854.000000	0	0	0
	0.5	0.002703	7875.284553	5	150	19.046931
2.02	1.0	0.005405	7896.684783	7	210	26.593438
4.14	1.5	0.008108	7918.201635	24	720	90.929738
5.17	2.0	0.010811	7939.836066	36	1080	136.02296
6.18	2.5	0.013514	7961.589041	46	1380	173.33223
7.18	3.0	0.016216	7983.461538	55	1650	206.67727
8.18	3.5	0.018919	8005.454545	63	1890	236.08903
9.18	4.0	0.021622	8027.569061	69	2070	257.86138
10.15	4.5	0.024324	8049.806094	76	2280	283.23664
10.15	5.0	0.027027	8072.166667	81	2430	301.03442
12.13	5.5	0.029730	8094.651811	86	2580	318.72897
13.18	6.0	0.032432	8117.262570	92	2760	340.01610
14.35	6.5	0.035135	8140.000000	99	2970	364.86486
15.38	7.0	0.037838	8162.865169	102	3060	374.86837
16.37	7.5	0.040541	8185.859155	105	3150	384.80994
17.35	8.0	0.043243	8208.983051	108	3240	394.68957
18.32	8.5	0.045946	8232.237960	109	3270	397.21884
19.29	9.0	0.048649	8255.625000	111	3330	403.36134
20.27	9.5	0.051351	8279.145299	113	3390	409.46256
21.25	10.0	0.054054	8302.800000	115	3450	415.52247
22.34	10.5	0.056757	8326.590258	115	3450	414.33527
23.31	11.0	0.059459	8350.517241	118	3540	423.92584
24.45	11.5	0.062162	8374.582133	119	3570	426.28993
25.47	12.0	0.064865	8398.786127	122	3660	435.77726
26.45	12.5	0.067568	8423.130435	123	3690	438.07941
27.45	13.0	0.070270	8447.616279	125	3750	443.91221
28.42	13.5	0.072973	8472.244898	125	3750	442.62177
29.4	14.0	0.075676	8497.017544	124	3720	437.80067
30.35	14.5	0.078378	8521.935484	124	3720	436.52055
31.32	15.0	0.081081	8547.000000	123	3690	431.73043
32.32	15.5	0.083784	8572.212389	123	3690	430.46064
33.36	16.0	0.086486	8597.573964	122	3660	425.70148
34.49	16.5	0.089189	8623.086053	122	3660	424.44201
35.52	17.0	0.091892	8648.750000	121	3630	419.71383
36.51	17.5	0.094595	8674.567164	121	3630	418.46468
37.47	18.0	0.097297	8700.538922	120	3600	413.76747

RESULTS AND DISCUSSION

Triaxial compression test: The graphical representation of the triaxial test results under a confining stresses of 200, 400, and 600 kPa for the sample is given in Fig. 2, 3 and 4. The experimental data for triaxial tests under confining stresses of 200 and 400 kPa are appended as Table 1 and 2, respectively.

From the Fig. (2, 3 and 4) shows the relationship of stress and strain, of which the behavior shows clearly how most engineering materials' curves behave. As the curve starts from zero it becomes linear until 10% strain, at this region it obeys Hooke's law.

After this point, the material starts to behave both elastic and plastic before it collapses. Each of the figures can therefore be effectively divided into three portions namely elastic region, elastic-plastic region and the plastic collapse region. These regions however, have no distinct boundaries.

The coefficient of determination, R², between the measured values and the fitted values were obtained as 0.9977521, 0.9856786 and 0.9978727, respectively as shown above. These were indicators that the measured data and the regressed values fitted quite closely statistically

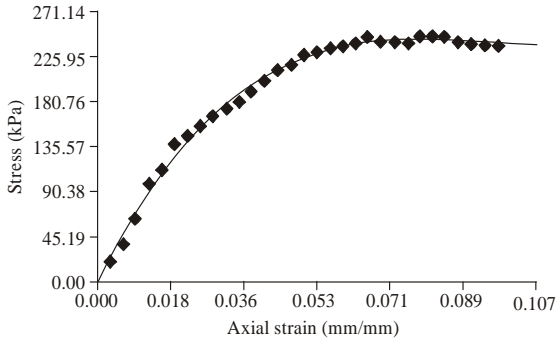


Fig. 2: Stress vs axial strain at confining stress of 200 kPa, 3rd degree Polynomial Fit: $y = a+bx+cx^2+dx^3...$; Coefficient Data, a: -1.5476399; b: 8350.0974; c: -92868.488; d: 333787.15; Standard Error: 5.1604425; Coefficient of determination, R^2 : 0.9977521

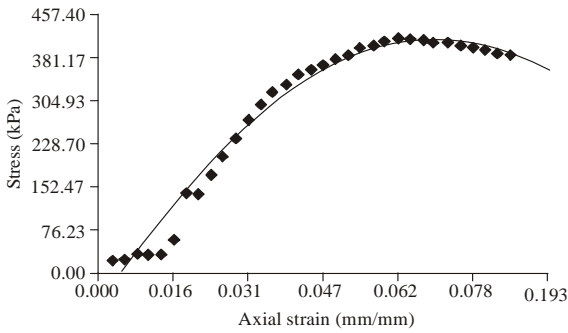


Fig. 3: Stress vs axial strain at confining stress of 400 kPa, Quadratic Fit: $y = a+bx+cx^2$; Coefficient Data, a: -62.195406; b: 13702.836; c: -98312.96; Standard Error: 26.2302973; Coefficient of determination, R^2 : 0.9856786

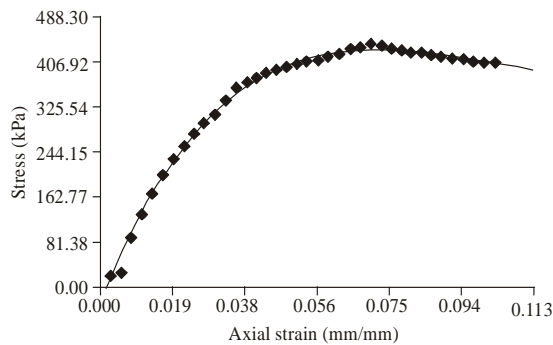


Fig. 4: Stress vs axial strain at confining stress of 600 kPa, 4th Degree Polynomial Fit: $y = a+bx+cx^2+dx^3...$; Coefficient Data: a: -25.665453; b: 17328.691; c: -222636.4; d: 1121486.4; e: -1893758.6; Standard Error: 9.0261499; Coefficient of determination, R^2 : 0.9978727

Mohr-coulomb failure: The Table 3 and Fig. 5 show the collapse stresses for bulk groundnuts sample under confining stresses; 200, 400 and 600 kPa.

Table 3: Collapse stresses (kPa) obtained from triaxial tester

	Confining stresses (kPa)	Collapse stresses (kPa)
1	200	246
2	400	356
3	600	443

Table 4: ANOVA analysis.

Source	SS	df	MS	F	Prob>F
Friction angle	12	2	6	1	0.42187
Error		13.5	6	2.25	
Total	18	8			

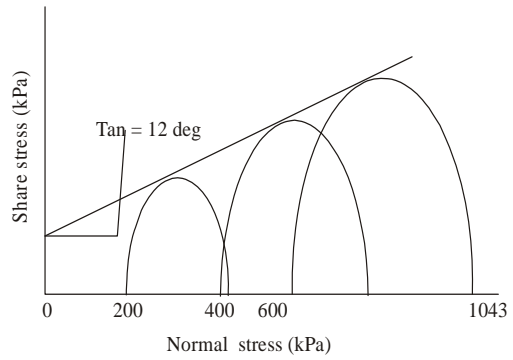


Fig. 5: Mohr-coulomb diagram ($Q' = 12 \phi^{\circ}C = 6.3 \text{ kPa}$) generated with AutoCad software

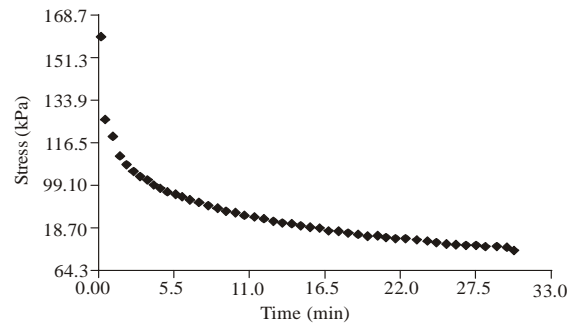


Fig. 6: Stress vs time, Standard error: 2.5406641; Correlation Coefficient $R^2 = 0.9856933$

The values obtained for the angle of internal friction was 12° and cohesion factor $c = 6.3 \text{ kPa}$ as defined by the Mohr-Coulomb failure envelope obtained from triaxial compression tests for bulk groundnuts under varying confining pressures.

A one-way ANOVA analysis of the above findings showed no significant difference between the different confining pressures with p-values of 0.4218. These findings at the 95% confidence level is given below:

One way ANOVA table for the means of angle of internal friction under the confining pressures; $p = 0.42187$ (Table 4).

Stress relaxation: The curve of the stress relaxation of the bulk groundnuts obtained from the experiment Table 5 and the Maxwell model curve are shown below in the Fig. 6 and 7, respectively.

Table 5: Table of stress and time for stress relaxation

Time (min)	Stress (kPa)	Time (min)	Stress (kPa)
0.1	160	16.0	82.0
0.5	125.8	16.5	81.2
1.0	118.8	17.0	80.8
1.5	110.8	17.5	80.8
2.0	107.4	18.0	79.8
2.5	105.0	18.5	79.6
3.0	102.6	19.0	79.6
3.5	101.6	19.5	78.6
4.0	99.60	20.0	78.4
4.5	98.00	20.5	78.4
5.0	97.00	21.0	77.4
5.5	95.80	21.5	77.2
6.0	94.60	22.0	77.1
6.5	93.40	22.5	77.1
7.0	92.34	23.0	77.0
7.5	92.08	23.5	77.0
8.0	91.12	24.0	76.4
8.5	90.00	24.5	76.2
9.0	89.14	25.0	75.2
9.5	88.88	25.5	75.0
10.0	87.60	26.0	75.0
10.5	86.80	26.5	75.0
11.0	86.60	27.0	75.0
11.5	86.40	27.5	75.0
12.0	85.40	28.0	74.0
12.5	84.20	28.5	74.0
13.0	84.20	29.0	74.0
13.5	84.20	29.5	74.0
14.0	84.00	30.0	73.0
14.5	83.00		
15.0	83.00		
15.5	82.00		

Table 6: Test for creep at constant stress $L_0 = 185$ mm

Elapsed time	Deformation dial, ΔL	Axial strain, (mm/mm)
0	0.0	0
1	0.5	0.002702703
2	1.0	0.005405405
3	1.5	0.008108108
4	2.0	0.010810811
5	2.5	0.013513514
6	3.0	0.016216216
7	3.5	0.018918919
8	4.0	0.021621622
9	4.5	0.024324324
10	5.0	0.027027027
11	5.5	0.029729730
12	6.0	0.032432432
13	6.5	0.035135135
14	7.0	0.037837838
15	7.5	0.040540541
16	8.0	0.043243243
17	8.5	0.045945946
18	9.0	0.048648649
19	9.5	0.051351351
20	10.0	0.054054054
21	10.5	0.056756757
22	11.0	0.059459459
23	11.5	0.062162162
24	12.0	0.064864865
25	12.5	0.067567568
26	13.0	0.070270270
27	13.5	0.072972973
28	14.0	0.075675676
29	14.5	0.078378378
30	15.0	0.081081081

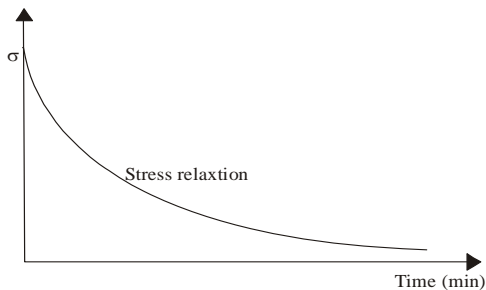


Fig. 7: Stress relaxation curve of the Maxwell model

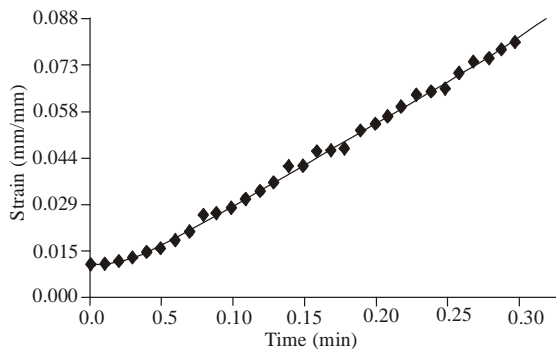


Fig. 8: Creep test, 5th Degree Polynomial Fit: $y = a + bx + cx^2 + dx^3$; Standard Error = 0.0012030; Correlation Coefficient $R^2 = 0.9989148$

Figure 6, shows stress relaxation of bulk groundnuts. The curve reduces exponentially as time increases. The behaviours of the curve have a close relationship with the Maxwell model. The Correlation Coefficient: $R^2 = 0.9856933$ which indicate the measured data and the regressed values fitted quite closely statistically.

The stress relaxation curve of the Maxwell model is as shown below:

Creep test: The curve of the creep test of the bulk groundnuts obtained from the experimental results appended in Table 6 is shown in the Fig. 8.

CONCLUSION

The findings have showed that bulk groundnuts behave like other engineering materials that display viscoelastic properties. As such, other approaches to the testing of materials such as the Mohr-Coulomb failure criterion can accurately be applied to this set of materials. Bulk groundnuts exhibited stress-strain behaviour that is consistent with other engineering materials.

Senstar test results obtained for bulk groundnuts provided the stress-relaxation curve similar to Maxwell viscoelastic model. These results showed that the

Maxwell model for viscoelastic polymers can be applied to accurately describe the behaviour of bulk groundnuts.

Creep results showed that bulk groundnuts exhibits same behavior as other engineering materials.

REFERENCES

- Aggrawal, K.K., B.L. Clary and E.W. Schroeder, 1973. Mathematical model of peanut pod geometry. *Transact. ASAE*, 16(2): 315-319.
- Ak, M. and S. Gunasekaran, 1992. Stress-Strain Curve Analysis of Cheddar Cheese under Uniaxial Compression. *J. Food Sci.*, 57: 1078 -1081.
- Bishop, A.W. and D.J. Henkel, 1962. The measurement of soil properties in the triaxial test. Edward Arnold Publishers, London.
- Chi, L., S. Tessier, E. Mckyes and C. Laque, 1993. Modelling mechanical behaviour of agricultural soils. *Transact. ASABE*, 36(6): 1563-1570.
- Goldhirsch, I. and C. Goldenberg, 2004. Stress in Dense Granular materials. In: Hinrichsen, H. and E.W. Dietrich, (Eds.), *The Physics of Granular media*. Wiley-VCH Verlag GmbH and Co. KGaA, Weinheim.
- Gumbe, L.O. and B.M. Maina, 1990. Elastoplastic constitutive parameters for rice *En-Masse*. *Afri. J. Sci. Technol. AJST publicat.*, 11(2).
- Mccrum, Buckley and Bucknell, 2003. *Principles of Polymer Engineering*. Pp: 117-176
- Meyers and Chawla, 1999. *Mechanical Behavior of Materials*. 1st Edn., Cambridge University Press, Cambridge.
- Moya, M., F. Ayuga, M. Guaita and P.J. Aguado, 2002. Mechanical properties of granular agricultural materials considered in silos design. Proceedings of the 15th ASCE Engineering Mechanics Conference, June 2-5, 2002, Columbia University, New York.
- Moya, M., F. Ayuga, M. Guaita and P.J. Aguado, 2006. Mechanical properties of granular agricultural materials, part 2. *Transact. ASABE*, 49(2): 479-489.
- Ndukwu, M.C., 2009. Determination of selected physical properties of *Brychystegia eurycoma* seeds. *RES. Agri. Eng.*, 55(4): 165-169.
- Oranga, E., 2005: Elastoplastic and viscoelastic behaviour of cohesionless shelled maize *en masse*. Msc. Thesis, Department of Environmental and Biosystems Engineering, University of Nairobi, Kenya,
- Wang, Q., D.E. Pufahl and D.G. Fredlund, 2002. A study of critical state on an unsaturated silty soil. *Can. Geotech. J.*, 39(1): 213-218.
- Wood, D.M., 1990. *Soil Behaviour and Critical State Soil Mechanics*. Cambridge University Press, UK, pp: 462.
- Zhang, Q., Y. Li, V.M. Puri and H.B. Manbeck, 1989a. Physical properties effect on stress-strain behaviour of wheat *en-masse*. Published by the American society of agricultural and biological engineers, St. Joseph, Michigan. *Transact. ASABE*, 32(1): 0203-0209.
- Zhang, Q., X. Bu and M.G. Britton, 1998. An analytical model for predicting stresses in grain storage bins. Published by the American Society of Agricultural and Biological Engineers, St. Joseph, Michigan. *Transact. ASAE*, 41(6): 1655-1661.
- Zhang, Q., Y. Li, V.M. Puri and H.B. Manbeck, 1986. Physical properties effect on stress-strain behaviour of wheat *en-masse*. Published by the American Society of Agricultural and Biological Engineers, St. Joseph, Michigan. *Transact. ASABE*, 32(1): 0194-0202.